

# Investigation of Laser Parameters in Silicon Pulsed Laser Conduction Welding

Mahdi Shayganmanesh<sup>1</sup> · Afsaneh Khoshnoud<sup>1</sup>

Accepted: 4 January 2016 / Published online: 13 January 2016  
© Springer Science+Business Media New York 2016

**Abstract** In this paper, laser welding of silicon in conduction mode is investigated numerically. In this study, the effects of laser beam characteristics on the welding have been studied. In order to model the welding process, heat conduction equation is solved numerically and laser beam energy is considered as a boundary condition. Time depended heat conduction equation is used in our calculations to model pulsed laser welding. Thermo-physical and optical properties of the material are considered to be temperature dependent in our calculations. Effects of spatial and temporal laser beam parameters such as laser beam spot size, laser beam quality, laser beam polarization, laser incident angle, laser pulse energy, laser pulse width, pulse repetition frequency and welding speed on the welding characteristics are assessed. The results show that how the temperature dependent thermo-physical and optical parameters of the material are important in laser welding modeling. Also the results show how the parameters of the laser beam influence the welding characteristics.

**Keywords** Pulsed laser · Silicon · Conduction welding · Laser beam characteristics

## Introduction

Nowadays laser welding is one of the important industrial applications of the laser. First practical demonstration of the laser welding was performed by Platte and Smith in 1963 which involved welding of stainless steel foils by pulsed ruby laser [1]. Principally laser welding are performed in two main modes; conduction and keyhole welding. Keyhole welding in which a vapor-plasma-filled cavity is formed is a deep welding and often used in welding thick-sheets of materials [2]. Laser keyhole welding is often referred to as a high energy density or power laser beam. However for thin layer of materials low

---

✉ Mahdi Shayganmanesh  
shaygan@iust.ac.ir

<sup>1</sup> School of Physics, Iran University of Science and Technology, Narmak, Tehran, Iran

energy (or power) density of laser beam is sufficient for welding which is referred to conduction welding. When the laser beam spot size is generally comparable to the thickness of the sheet or laser intensity is insufficient to boil the materials, the conduction welding mode is likely to be encountered [3]. In laser welding there is not a sharp transition between conduction mode and keyhole mode. The minimum power density to initiate a keyhole in metals is approximately  $10^6$  W/cm<sup>2</sup>. Below this power density threshold a conduction welding mechanism will occur [4].

In parallel to experimental research, theoretical investigations and modeling were also in progress for characterization and optimization of laser welding. Pioneering models for laser welding are introduced by Steen et al. [5, 6]. One of the first numerical solutions of heat transfer for laser materials processing was due to Mazumder and Steen [5] who produced a 3-D model using Finite Difference techniques and a relaxation procedure in solving the heat conduction equation. They assumed a CW laser with Gaussian beam, a workpiece of infinite length, 100 % absorption of power at temperatures in excess of the boiling point, radiation heat losses and also convective heat losses due to the shielding gas flow. Mohanty and Mazumder [7] produced a 3-D numerical keyhole welding simulation model with graphical user interface and visualization modules.

A comprehensive literature survey on laser welding and related process is provided by Mackwood and Crafer in 2005 [8].

Verhaeghe and Hilton [9] investigated the effects of laser beam quality and spot size on the welding performance experimentally with CW laser for aluminium and steel. They showed how the laser beam quality of CW lasers affects welding performance, by comparing a series of welds made in thin and thick section aluminium and steel. Also Balasubramanian et al. [10] studied the effects of beam power, welding speed and beam angle on the welding characteristics numerically and experimentally. They as well considered some temperature depended thermo-physical parameters of the material. However the material of workpiece in their work were stainless steel and they used CW Nd:YAG laser for deep penetration welding. More recently Duocastella and Arnold investigated Bessel beams for material processing. They have shown that laser beam profile has important effect in laser material processing [11]. Daniel et al. studied the effects of Q-switched diode pumped solid state laser on silicon [12]. Although they considered pulsed laser and pulse related parameters in their investigations, other laser parameters such as polarization and laser beam quality are not investigated in their work. Also in that work they concentrated on mass removal by laser. Furthermore Assuncao et al. [4] investigated interaction time and beam diameter effects on the conduction mode limit. But they considered CW laser in their work.

In literature generally the welding of metals were considered, though in recent years laser welding of special alloys and dissimilar materials are more investigated. However in this paper welding of silicon is considered and the influence of different laser parameters on the welding characteristics are investigated. Although there are many differences between metals and semiconductors in atomic level, however it should be noted that in modeling of laser welding of bulk materials the thermal effects are under consideration and therefore the thermo-physical and optical parameters of the material are crucial.

Consequently the presented model in this paper can be extended to the welding of metals. The reason of choosing silicon workpiece is related to the silicon applications. Silicon welding has many recent applications in micro-electronic and electro-mechanic devices such as IC packaging also in photovoltaic (solar cell) manufacturing [13–15]. In the micro-mechanics and photovoltaic applications, thin sheets of silicon are used, therefore conduction welding is needed [14, 15].

To the best of our knowledge, there are a few reports on modeling of conduction welding of silicon by laser [14, 16]. However in none of them the laser parameters affecting the welding are investigated. In this work effects of spatial and temporal laser parameters such as beam spot size, beam quality, polarization, laser incident angle, laser pulse energy, pulse width and pulse repetition frequency on the welding characteristics are assessed. In this paper the heat conduction equation is solved in four dimensions, i.e., three spatial and one temporal dimension. In this work laser heat source is considered as a boundary condition, which simplifies the calculations. To increase the accuracy, all the thermo-physical and optical properties of the material are considered to be temperature dependent in our calculations. The effect of the movement of the workpiece (welding speed) is also studied in this paper.

A computational code is developed in MATLAB software and heat conduction equation is solved numerically using finite difference method in four dimensions. To validate our calculations, we have compared our results to those from other models and experiments. The results of this paper can be used in the characterization of silicon laser welding in conduction mode.

## Theory and the Model

In order to predict thermal effects of laser radiation on the workpiece in laser welding process, heat conduction equation should be solved to find the temperature distribution in the workpiece. Time depended heat conduction equation is given by relation (1) [17]:

$$\frac{\partial^2 T}{\partial x^2} + \frac{\partial^2 T}{\partial y^2} + \frac{\partial^2 T}{\partial z^2} + \frac{q}{K} = \frac{1}{\alpha} \frac{\partial T}{\partial t} \quad (1)$$

In which  $T=T(x,y,z,t)$  is the temperature at spatial and time coordinates  $x,y,z,t$  respectively,  $q$  is the rate of internal heat generation per unit volume,  $K$  is the thermal conductivity and  $\alpha$  is the thermal diffusivity.

In laser welding, laser energy absorbed by the workpiece serves as the heat source. In this work, the heat source is intended as a boundary condition. This is a result of assuming conduction mode welding. The boundary condition at the top surface of the workpiece regarding to the absorbed laser power, surface radiation and convection are as follows [10]:

$$q_{abs} - q_{rad} - q_{conv} = -K \frac{\partial T(x,y,z,t)}{\partial z} \Big|_{z=0} \quad (2)$$

In which  $q_{abs}$  is the laser absorbed intensity at the top surface of the workpiece,  $q_{rad}$  is the radiated intensity and  $q_{conv}$  is the power density loss due to the convection which are given by below relations [17]:

$$\begin{aligned} q_{abs} &= [1-R(x,y,0,t)]I(x,y,0,t) \\ q_{rad} &= \sigma \varepsilon (T^4(x,y,0,t) - T_\infty^4) \\ q_{conv} &= h (T(x,y,0,t) - T_\infty) \end{aligned} \quad (3)$$

In them  $\varepsilon$  is the thermal radiation coefficient,  $\sigma$  is the Stefan-Boltzmann constant and  $h$  is the convection heat transfer coefficient.  $T_\infty$  is the ambient temperature.  $R(x,y,0,t)$  is the reflectivity of surface of workpiece which is a function of time. When the laser hits the workpiece temperature rises with time, so the reflection coefficient varies. Therefore, reflectivity is shown as a function of time.  $I(x,y,0,t)$  is the intensity of incident laser on the workpiece as a function of position and time. Indeed for a pulsed laser, the boundary condition (relation (2)) is a function of time.

Incident laser beam is considered to have a quasi-Gaussian intensity profile. Quasi-Gaussian mode is a spatial profile which is not exactly the Gaussian mode, but can be approximated with negligible error by Gaussian model [18]. Therefore the laser intensity distribution is given by relation (4) [19]:

$$I(x,y,0) = \frac{p}{2\pi w^2} \exp\left(-\frac{x^2 + y^2}{2w^2}\right) \quad (4)$$

In which  $p$  is the maximum power of the laser beam and  $w$  is the radius of the laser beam profile [19].

As it is shown in Fig. 1, Laser beam can be transmitted to the workpiece by a beam delivery system which may consist of a fiber or some optical components in an arm.

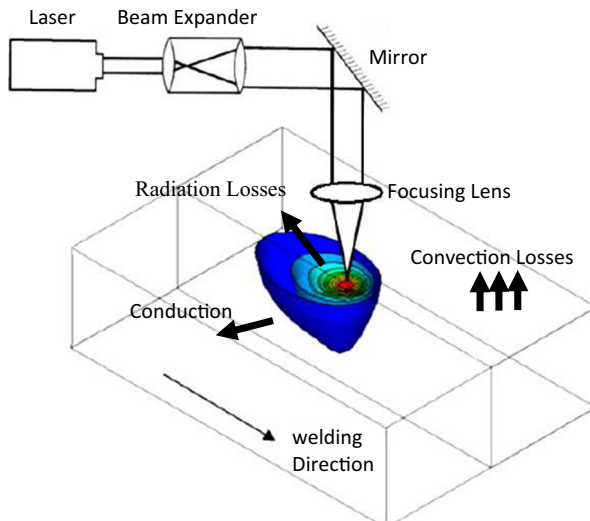


**Fig. 1** Schematic drawing of laser welding system; consist of laser, beam delivery subsystem, the workpiece and heat transfer mechanisms

After all, the beam will be focused on the workpiece by a lens. The beam spot size on the workpiece can be given by below relation [20]:

$$w = M^2 \frac{4\lambda f}{\pi D} \quad (5)$$

In which  $M^2$  is the beam quality factor,  $\lambda$  is the laser wavelength,  $f$  is the focal length of the lens used for focusing the beam on the workpiece and  $D$  is the radius of the incident beam on the lens [20].

The absorption of incident laser beam at the surface of silicon workpiece is dependent upon the incident angle and the polarization of the laser beam. The reflectance of the workpiece surface can be given by Fresnel relations for s and p polarizations [21]:

$$R_p = \frac{[n - (1/\cos\phi)]^2 + k^2}{[n + (1/\cos\phi)]^2 + k^2} \quad (6)$$

$$R_s = \frac{[n \cos\phi]^2 + k^2}{[n + \cos\phi]^2 + k^2} \quad (7)$$

In which  $n$  and  $k$  are real and imaginary parts of refractive index of the workpiece material respectively and  $\phi$  is incident angle of the laser beam. Having reflectance of workpiece surface, the absorption coefficient of the surface can be achieved directly by  $A = 1 - R$ .

In our calculations thermo-physical and optical properties of silicon are considered to be temperature dependent as it is shown in Table 1. As it is presented in Table 1, density and heat capacity are given with different functions for temperatures below and

**Table 1** Thermo-physical and optical properties of silicon (in SI units) as a function of temperature,  $T_m$  is the melting temperature of the silicon [22–27]

Temperature-dependent properties	
$\rho(T) = \begin{cases} 2.311 \times 10^3 - 2.63 \times 10^{-2}(T - T_m) \\ 2.580 \times 10^3 - 0.171(T - T_m) - 1.61 \times 10^{-4}(T - T_m)^2 \end{cases}$	$T \leq T_m$ $T > T_m$
$K(T) = \frac{29900}{(T - 99)}$	
$C_p(T) = \begin{cases} \left(\frac{10^6}{\rho(T)}\right) \left(1.4743 + \frac{0.17066T}{300}\right) \\ \frac{2.432 \times 10^6}{\rho(T)} \end{cases}$	$T \leq T_m$ $T > T_m$
$\alpha(T) = \frac{128}{10^4(T - 159)}$	
$n(T) = n_0 + \frac{C_n(T - T_R)}{2n_0}$	
$k(T) = k_0 e^{C_k(T - T_R)}$	$T_R = 29 \text{ } ^\circ\text{C}$

above the melting point [22–27]. In the next section, the results of our calculations are presented.

## Results and Discussions

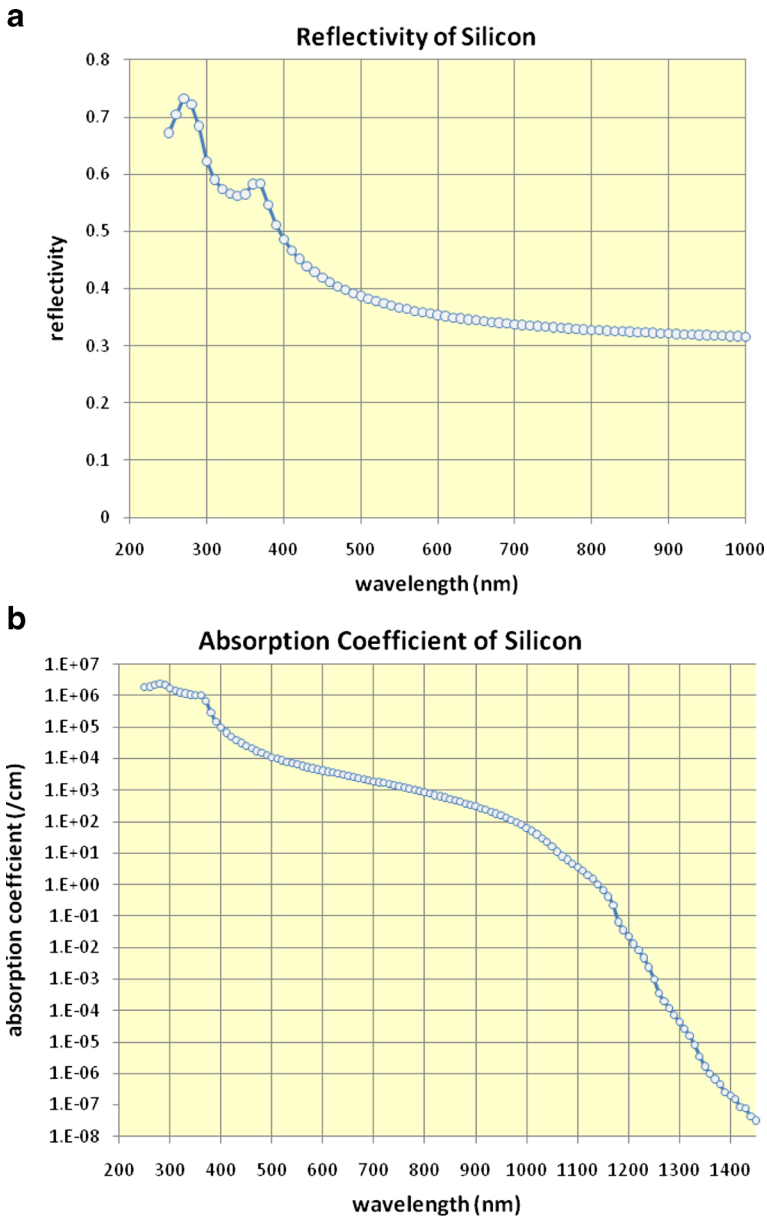
To select the appropriate wavelength for the laser source in silicon welding, in addition to the existence of such a laser, the reflectivity of silicon for that wavelength should be considered. Lower reflectivity of the workpiece surface leads to the better absorption of the laser and in turn leads to increasing welding efficiency. As it is shown in Fig. 2a [28], for the wavelengths more than 500 nm the silicon reflectivity is less than 40 % which is acceptable.

Figure 2b shows the spectral absorption coefficient of silicon [28]. As it is seen in the figure, the magnitude of absorption coefficient is extremely high in UV and visible ranges of the spectrum. For example in wavelengths of 300 and 500 nm the absorption coefficients are  $10^6$  and  $10^4 \text{ cm}^{-1}$  respectively. Therefore the skin depth of the silicon for visible and UV wavelengths is very low; this means that laser energy will be absorbed in a very thin layer of silicon at the surface. In other words taking into account laser beam energy as a boundary condition is true even conceptually. The calculations of this paper are conducted for wavelength of 808 nm in which also the skin depth is small enough. This wavelength can be achieved by a typical GaAs diode laser [29]. As it is shown in the Fig. 2b for the wavelength of 808 nm the absorption coefficient of silicon is about  $10^3 \text{ cm}^{-1}$  which leads to the skin depth of 0.001 cm or 10  $\mu\text{m}$ . In this work the thickness of the silicon is considered to be about 400  $\mu\text{m}$ , therefore the mentioned assumption is fulfilled.

The dimensions of the workpiece are assumed to be  $0.11 \times 0.11 \times 0.04$  cm. Also the number of mesh points in x,y and z directions are  $55 \times 55 \times 27$  respectively. The discrete time steps in the code is considered to be  $dt = 5 \times 10^{-4}$  msec. Also the parameters of the laser are presented in Table 2. Based on the equations in the previous section, thermal interaction of the laser and silicon workpiece is modeled and the temperature distribution in the silicon is calculated for different laser parameters. Having temperature distribution, the melt pool profile is achieved and welding is characterized.

In Fig. 3 the temperature dependence of thermo-physical and optical properties of silicon are shown relatively. As it is shown in the figure, thermal conductivity, thermal diffusivity and reflectivity are strongly temperature dependent and it must be considered in calculations. But density and heat capacity varies slowly by temperature. However we assumed that all the mentioned parameters are temperature dependent in our calculations.

In Fig. 4 the effect of temperature dependence of thermo-physical and optical parameters of material on the maximum temperature of the workpiece are shown. In Fig. 4a maximum temperature in different depths of the workpiece is presented for two cases; temperature depended and constant thermo-physical and optical parameters. As it is seen in the figure the difference of the two cases is only important for points near the top surface of the workpiece. For points in the depth, the temperature dependence of the parameters can be ignored. Figure 4b shows maximum temperature of the workpiece for temperature depended and constant thermo-physical and optical parameters in compare of experimental results from other researchers [16]. In this special figure to



**Fig. 2** a) Reflectivity of silicon versus wavelength b) Spectral absorption coefficient of silicon [28]

compare result of this study with the others the magnitude of laser parameters have been considered as those in reference [16]. This figure shows that considering temperature dependence thermo-physical and optical parameters leads to the results which are more similar to experiment.

The validity of our calculations is verified in two manners; in the first way, the one-dimensional limiting case of temperature of the workpiece is investigated. The height and the width of the workpiece are assumed to be too small and then temperature

**Table 2** Laser parameters used in the simulations

Laser mode	Pulsed
Laser wavelength (nm)	808
Pulse repetition frequency (kHz)	10–25
Pulse width ( $\mu\text{s}$ )	25
Laser energy per pulse (mJ)	7
Laser beam quality $M^2$	1–2
Laser temporal pulse shape	Rectangular

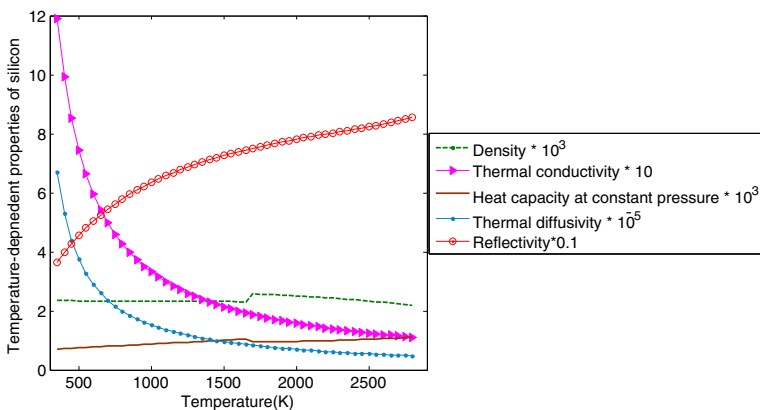
distribution of the workpiece is compared to the temperature distribution in a wire (one dimensional) which there is analytical solution for it. Analytical solution for heat conduction equation in a wire (one dimensional workpiece) can be given by [30]:

$$0 < x < L, T(x, 0) = T_0, T(x, \infty) = T_1$$

$$\frac{T(x, t) - T_1}{T_0 - T_1} = \frac{2}{\pi} \sum_{n=1}^{\infty} \frac{1 - (-1)^n}{n} \sin\left(\frac{n\pi x}{L}\right) \exp\left(-\frac{n^2 \pi^2 \alpha t}{L^2}\right) \quad (8)$$

In which  $T_0$  is the initial temperature of wire and  $T_1$  is the boundary temperature (temperature  $T_0$  at two end of the wire). The numerical solution is achieved by our developed numeric code. The height and width of the workpiece are assumed to be too small in compare of the length of workpiece. Figure 5a shows this comparison between analytical and numerical calculated temperature in different times which are in complete agreement. In second method, we compared maximum temperature of workpiece to those of others [16]. Figure 5b shows this verification. As can be seen, there is an acceptable agreement between two presented diagrams. It must be noted that thermo-physical and optical properties are assumed to be constant in the calculations of Fig. 5b.

Another parameter affecting the welding characteristics is the spot size of the focused laser beam on the workpiece. Fig. 6 shows the temperature distribution in

**Fig. 3** Thermo-physical and optical parameters of silicon (in SI units) versus temperature



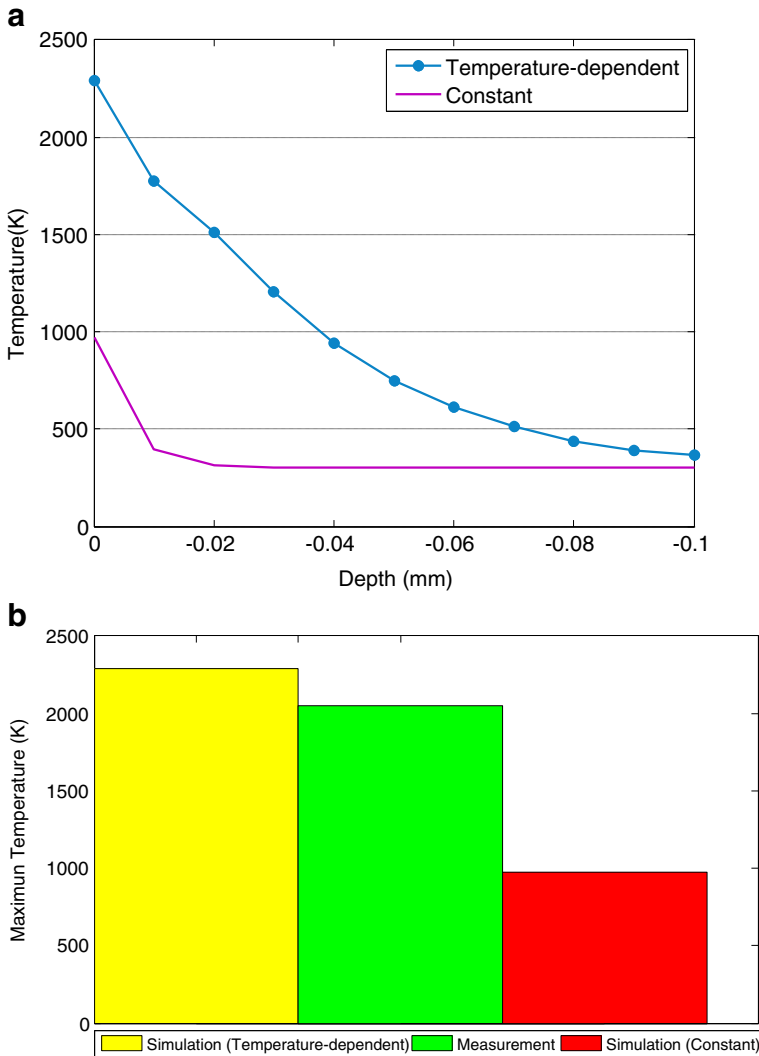


**Fig. 4** a) Calculated maximum temperature in each depth of workpiece for constant and temperature depended thermo-physical and optical parameters b) Maximum temperature of workpiece for constant and temperature dependent thermo-physical and optical properties in compare of experimental data from reference [16]

the workpiece for different beam spot sizes. Due to the symmetry in the weld pool profile, Fig. 6 is plotted in two dimensions. The parameter  $d/w$  in which  $d$  is the depth of the weld pool and  $w$  is the width of the weld pool, is used to characterize the weld pool geometry. Figure 7 shows the magnitude of  $d/w$  parameter versus beam spot size on the workpiece. As it is seen in the figure, decreasing the beam size leads to the deep and narrow weld pools. By decreasing the laser beam size while maintaining other parameters such as laser energy and pulse repetition frequency, the intensity of laser on the workpiece increases which leads to deeper weld. This can be explained via intensity related boundary condition (relation (2)). By increasing intensity, the gradient of the

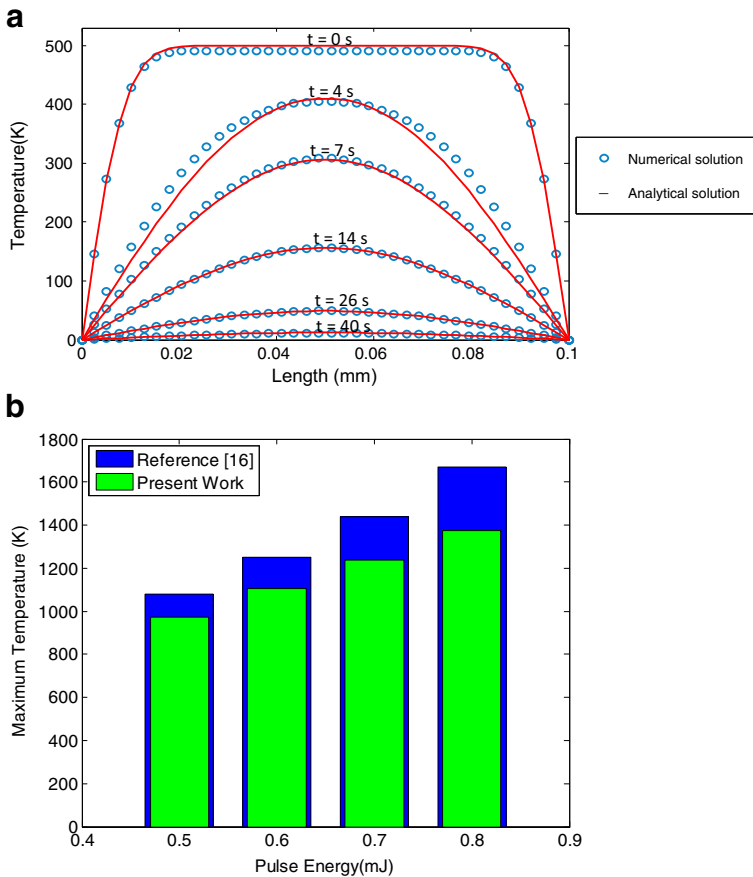


**Fig. 5** a) Numerical calculated temperature distribution in workpiece in the one dimensional limiting case in compare of analytical result b) Maximum temperature of workpiece versus laser pulse energy calculated from our model in compare of data from reference [16]

temperature on the surface increases and this leads to the increasing temperature of points in greater depth due to the conduction. From the other hand by reducing the laser beam size, laser affected area at the upper surface of the workpiece decreases leading to the decrease of weld width. Therefore deep and narrow weld pool is formed with decreasing the laser beam size.

Generally in the presented curves when one parameter is changed, the other parameters kept the same. In this way the effect of changing just that parameter on the welding characteristics is evaluated. For example when the beam spot size is varied, laser pulse energy as well as other parameters remained the same.

One of the important parameters of the laser beam is the beam quality factor. The beam quality factor which is called the  $M^2$  determines the focusability of the beam. In Fig. 8 maximum temperature of the workpiece is plotted versus  $M^2$  parameter. As Fig. 8 shows, approximately 50 % increase in  $M^2$  leads to less than 50 % decrease in maximum temperature of the workpiece. In another word increasing  $M^2$  decreases nonlinearly the maximum temperature of weld. This shows that  $M^2$  factor is a very important parameter in laser welding characterization and should be chosen

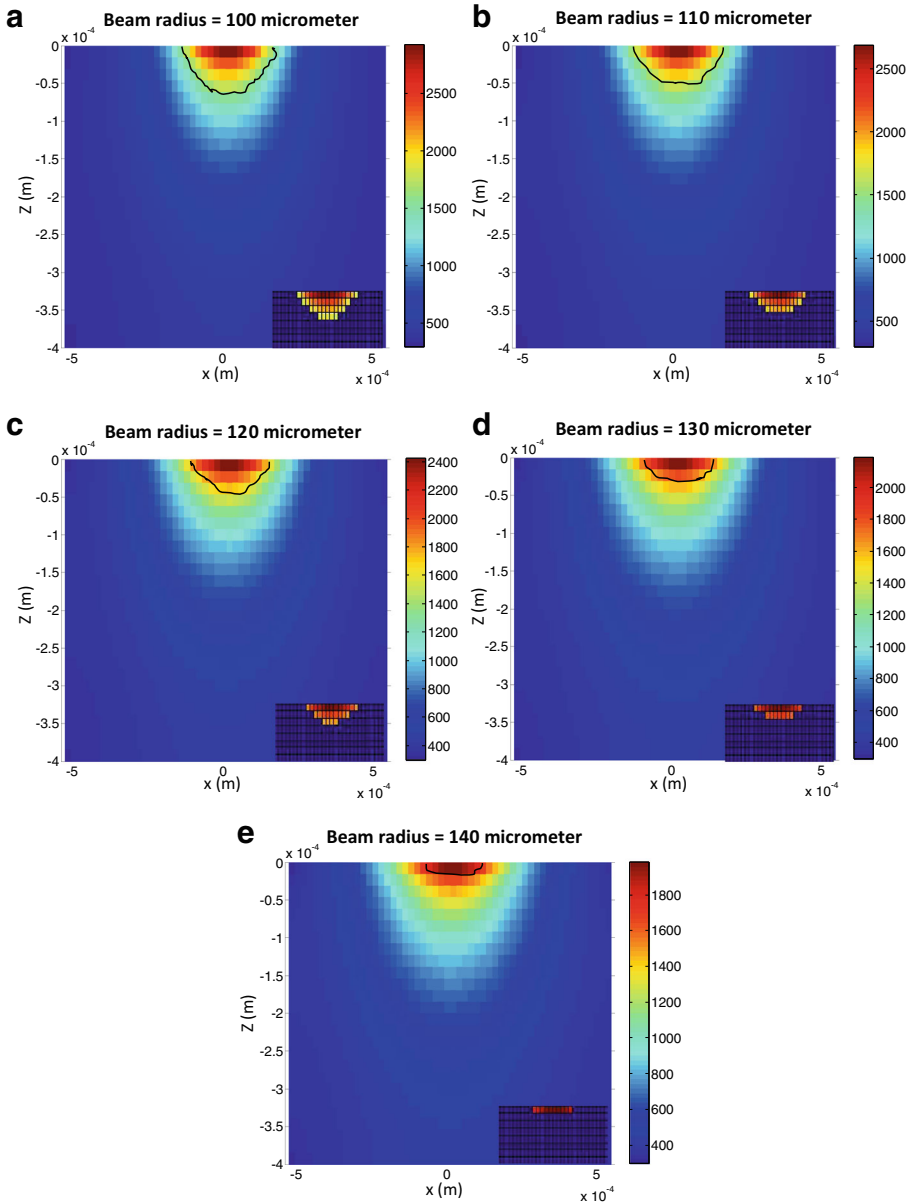


**Fig. 6** Two dimensional contour of temperature distribution in the workpiece for different beam spot sizes. In bottom right of each figure the weld pool is shown

appropriately. Usually in a laser, the laser output power and beam quality are not completely independent to each other (at least in a wide range changes of output power). However it must be noted that in this work we have tried to evaluate the effect of each parameter of the laser separately on the weld. Accordingly only the changes of the laser beam quality is considered in Fig. 8. Also it must be noted that in practice one need to find certain values for power and beam quality of the laser for

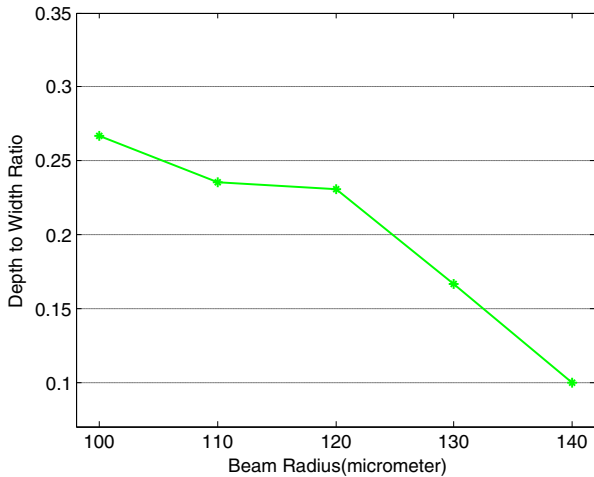


Fig. 7 Depth to width ratio ( $d/w$ ) of the weld pool versus beam spot size

appropriate welding. In this situation, Fig. 8 shows the sensitivity of the maximum temperature to the changes of the beam quality.

Another important parameter of the laser beam is polarization. Absorption coefficient of the laser beam depends on the polarization. Therefore it is expected that welding specifications also be dependent to the polarization of the laser beam. To check the mentioned dependence, in Fig. 9 maximum temperature in each depth of the workpiece is shown for different laser beam polarization and different angle of incidence (angle between the incident beam and the normal to surface of workpiece). This figure shows that in the same conditions, there is a serious different between induced

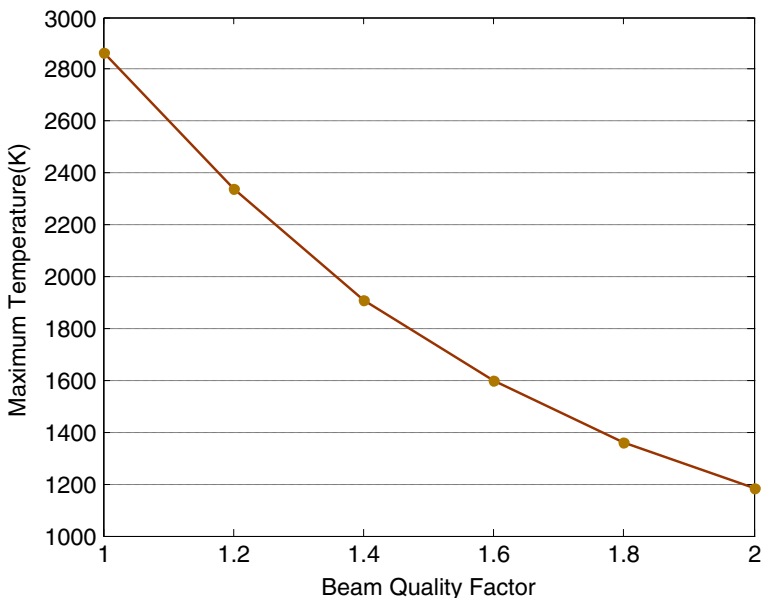
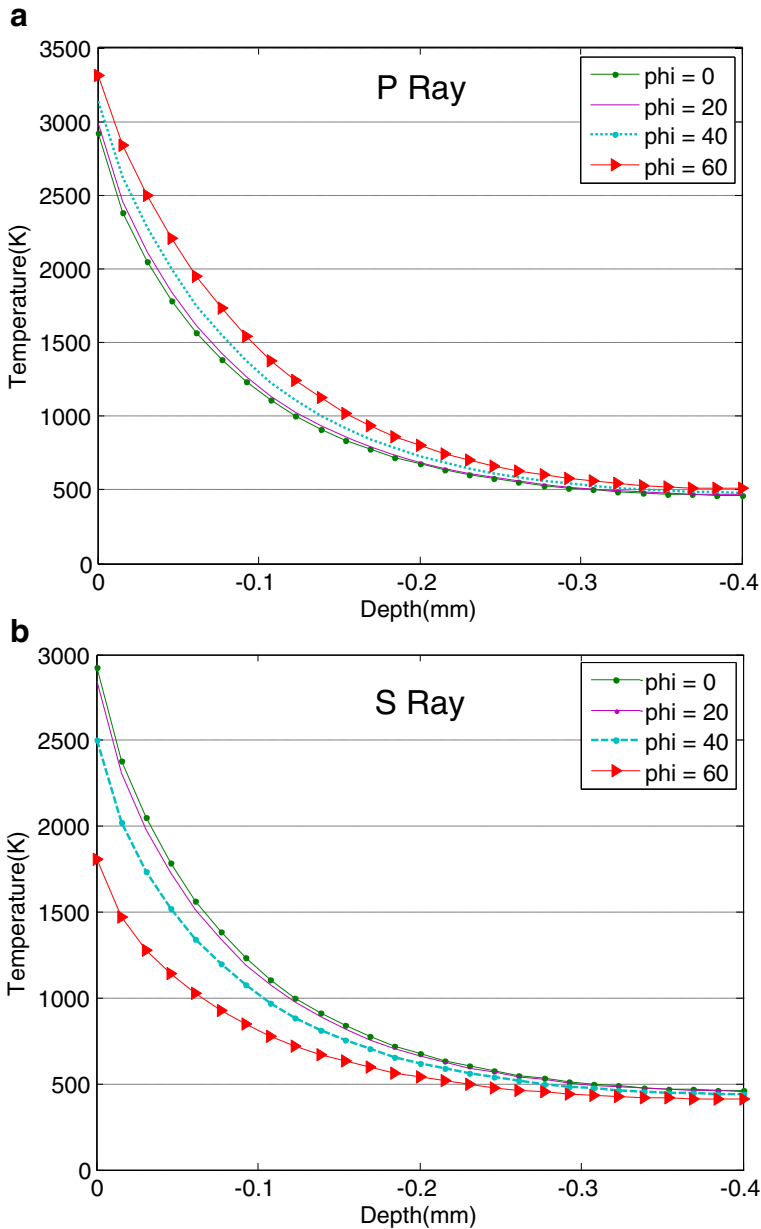
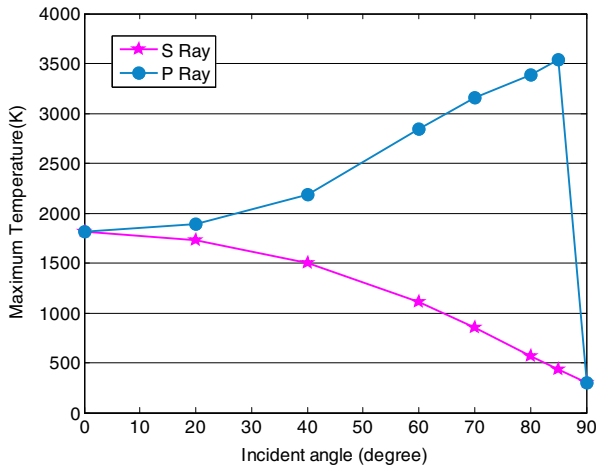


Fig. 8 Maximum temperature of the workpiece versus laser beam quality factor



**Fig. 9** a) Maximum temperature in each depth of the workpiece for laser beam with p polarization and for different incident angle b) Same as (a) but for s polarization

temperature for s and p polarizations. In some practical situations due to the special geometry of the workpiece, normal (vertical) radiation of laser beam is impossible, and the workpiece must be irradiated with the laser beam obliquely. As it is shown in Fig. 9, in obliquely radiation welding, p polarization generates higher temperatures and therefore it is better than s polarization. Also the difference of temperatures for p and



**Fig. 10** Maximum temperature of the workpiece versus laser incident angles for s and p polarization

s polarization is noticeable in the surface of workpiece; nevertheless at the depth of workpiece effects of s and p polarizations are indistinguishable. This behavior can be seen for different angle of incidence.

To find the optimum angle of incidence for each polarization, maximum temperature of workpiece versus incident angle is shown in Fig. 10. Optimum angle of incidence is an angle in which the absorption of laser beam to the workpiece is maximized and therefore the induced temperature in the workpiece is maximized. As it is shown in the figure optimum angles of incidence for p and s polarizations are  $85^\circ$  and  $0^\circ$  respectively. In these situations optimum angle of incidence can be found by presented diagrams.

As it is mentioned in the previous section, in this paper calculations are conducted in four dimensions in which there are three spatial dimensions and one temporal dimension. Therefore it is possible to investigate changes of temperature in the workpiece by time. Figure 11 shows the maximum temperature of the workpiece versus time. As it is shown in the figure, maximum temperature changes fast by time. In the calculations

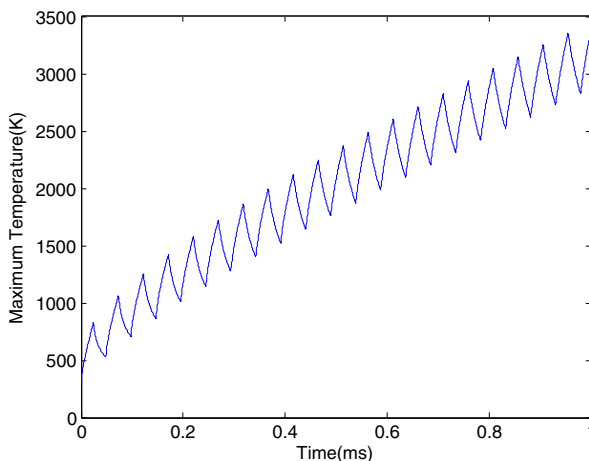


**Fig. 11** Maximum temperature of the workpiece versus time

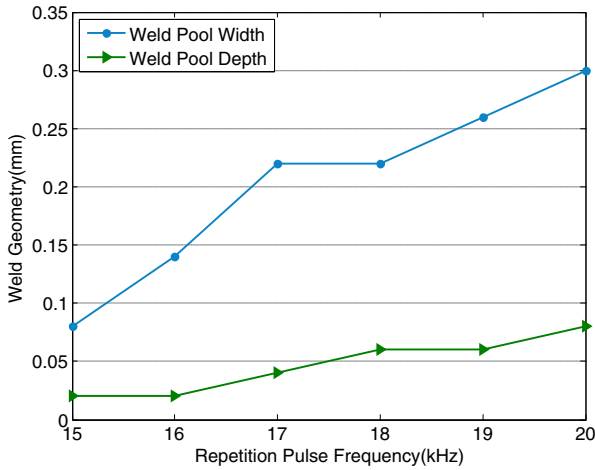


**Fig. 12** Dependence of weld pool geometry to the pulse repetition rate

relating to this figure, a pulsed laser is considered for welding. The pulse shape is considered to be rectangular shape versus time and with the 20 kHz repetition rate. As it is seen in the Fig. 11 the rate of the temperature changes is in the order of the repetition rate frequency of laser source. Although the temperature is oscillating but the average temperature rises by time.

To investigate the effect of pulse repetition rate of the laser on the weld profile, calculations are conducted for different repetition frequencies, and the weld depth and width are presented in Fig. 12. As it is seen in Fig. 12, by increasing repetition frequency, both of the depth and the width of the weld are increased. However the slope of the curve associated with width is more than that of depth. Therefore by increasing pulse repetition frequency, the  $w/d$  of the weld pool increases.

The last parameter of welding which is investigated in this paper is the welding speed. Movement of workpiece (or laser) decreases induced heating effect in the workpiece. Figure 13 shows the maximum temperature of the workpiece versus

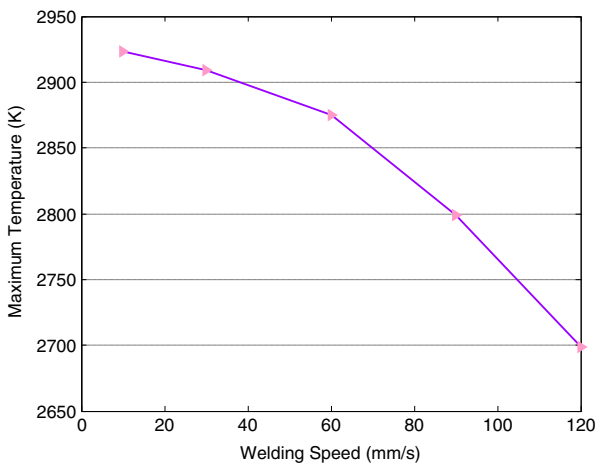


**Fig. 13** Maximum Temperature of the workpiece versus welding speed

welding speed. As it is seen in Fig. 13, by increasing the welding speed, maximum temperature of the workpiece is reduced. This is because that by increasing the welding speed, effective time exposure of the workpiece to the laser decreases. Moreover the profile of the weld changes when the laser beam and workpiece move to each other. Indeed welding speed break the symmetry of the weld pool. This can be physically explained. When the workpiece moves (or the beam scans the workpiece), in the direction of movement, the material is in a shorter time in the exposure of the laser radiation. However in the perpendicular direction the material is in longer time in exposure of laser radiation. This breaks the symmetry and this can also be explained by writing the heat conduction equation for moving workpiece. Considering chain derivation and neglecting heat source term, Eq. (1) changes to Eq. (9) as follows:

$$\frac{\partial T}{\partial t} = \frac{\partial T}{\partial x} \frac{dx}{dt} = -v \frac{\partial T}{\partial x} \quad (9)$$

$$\frac{\partial^2 T}{\partial x^2} + \frac{\partial^2 T}{\partial y^2} + \frac{\partial^2 T}{\partial z^2} = -\frac{v}{\alpha} \frac{\partial T}{\partial x}$$

In which  $v$  is the welding speed. As it is seen in the Eq. (9) the symmetry of equation in  $x$  and  $y$  directions is broken. In the direction of the workpiece movement which is supposed to be in  $x$  direction, the parameter  $v$  exist but not in the  $y$  direction.

As explained in this paper, effects of all laser parameters on the welding can be predicted by the presented model. This prediction can be used in optimization of silicon foil welding by laser as well as other conduction laser welding.

## Conclusions

In this paper the effects of laser parameters in laser welding are investigated numerically by solving the heat conduction equation. The parameters which are evaluated in this paper includes; laser beam spot size on the work piece,  $M^2$  factor, laser beam polarization and angle of incidence, laser pulse repetition frequency and the welding speed. Effects of the mentioned parameters on the maximum temperature of the workpiece and weld pool geometry are investigated in this paper and the results are presented. The results of our calculations can be useful in characterization and optimization of conduction laser welding.

## References

1. Platte, W.N., Smith, J.F.: Laser techniques for metals joining. *Weld. J.* **42**(11), 481–489 (1963)
2. Walsh, C.A.: LASER WELDING - Literature Review. Materials Science and Metallurgy Department, University of Cambridge, England (2002)
3. Noaker, P.M.: Lasers penetrate fabricating. *Manuf. Eng.* **10**, 33–40 (1993)
4. Assuncao, E., Williams, S., Yapp, D.: Interaction time and beam diameter effects on the conduction mode limit. *Opt. Lasers Eng.* **50**(6), 823–828 (2012)
5. Mazumder, J., Steen, W.M.: Heat transfer model for cw laser material processing. *J. Appl. Phys.* **51**, 941–947 (1980)



6. Steen, W.M., Dowden, J., Davis, M., Kapadia, P.: A point and line source model of laser keyhole welding. *J. Phys. D. Appl. Phys.* **21**(8), 1255 (1988)
7. Mohanty, P.S., Mazumder, J.: Workbench for keyhole laser welding. *Sci. Technol. Weld. Join.* **2**, 133–138 (1997)
8. Mackwooda, A.P., Crafer, R.C.: Thermal modeling of laser welding and related processes: a literature review. *Opt. Lasers Technol.* **37**, 99–115 (2005)
9. Verhaeghe, G., Hilton, P.: The effect of spot size and laser beam quality on welding performance when using high-power continuous wave solid-state lasers. *ICALEO 2005, 24th International Congress on Applications of Lasers & Electro-Optics* (2005)
10. Balasubramanian, K.R., Siva Shanmugam, N., Buvanashakaran, G., Sankaranarayanan, K.: Numerical and experimental investigation of laser beam welding of AISI 304 stainless steel sheet. *Adv. Prod. Eng. Manag.* **3**(2), 93–105 (2008)
11. Duocastella, M., Arnold, C.B.: Bessel and annular beams for materials processing. *Laser Photonics Rev.* **6**(5), 607–621 (2012)
12. Daniel, J.L., Hyungson, K., Jyoti, M.: Mass removal modes in the laser ablation of silicon by a Q-switched diode-pumped solid-state laser (DPSSL). *J. Phys. D. Appl. Phys.* **39**, 2624–2635 (2006)
13. Luo, C., Lin, L.: The application of nanosecond-pulsed laser welding technology in MEMS packaging with a shadow mask. *Sensor Actuator A* **97–98**, 398–404 (2002)
14. Heßmann, T.M.: *Laser Welding of Silicon Foils for Thin-Film Solar Cell Manufacturing*. Dissertation, Universität Erlangen (2014)
15. Brettschneider, T., Dorrer, C., Bründel, M., Zengerle, R., Daub, M.: Wafer-level packaging and laser bonding as an approach for silicon-into-lab-on-chip integration. *J. Micromech. Microeng.* **23**(5), (2013)
16. Tangwarodomnukun, V.: *Towards damage-free micro-fabrication of silicon*. Doctoral Dissertation, School of Mechanical and Manufacturing Engineering, the University of New South Wales (2012)
17. Holman, J.P.: *Heat Transfer*, 10th edn. McGraw-Hill, New York (2010)
18. Sun, H.: *A Practical Guide to Handling Laser Diode Beams*. Springer, Netherlands (2015)
19. Dowden, J.M.: *The Mathematics of Thermal Modeling*. Chapman & Hall/CRC (2001)
20. Hodgson, N., Weber, H.: *Laser Resonator and Beam Propagation*, 2nd edn. Springer Science+Business Media, Inc, New York (2005)
21. Reitz, J.R., Milford, F.J., Christy, R.W.: *Foundations of Electromagnetic Theory*, 4th edn. Addison-Wesley, Boston (1993)
22. Ohsaka, K., Chung, S.K., Rhim, W.K., Holzer, J.C.: Densities of Si determined by an image digitizing technique in combination with an electrostatic levitator. *Appl. Phys. Lett.* **7**(4), 423–425 (1997)
23. Touloukian, Y.S., Buyco, E.H.: *Thermophysical Properties of Matter*, vol. 2. IFI/Plenum, New York (1970)
24. Touloukian, Y.S., Makita, T.: *Thermophysical Properties of Matter*, vol. 6. IFI/Plenum, New York (1976)
25. Grigoropoulos, C.P., Buckholz, R.H., Domoto, G.A.: A heat transfer algorithm for the laser-induced melting and recrystallization of thin silicon layers. *J. Appl. Phys.* **60**, 2304–2309 (1986)
26. Moody, J.E., Hendl, R.H.: Temperature profiles induced by a scanning cw laser beam. *J. Appl. Phys.* **53**(6), 4364–4371 (1982)
27. Bergmann, J., Heusinger, M., Andr, G., Falk, F.: Temperature dependent optical properties of amorphous silicon for diode laser crystallization. *Opt. Express* **20**(S6), A856–A863 (2012)
28. <http://pveducation.org/pvcdrom/materials/optical-properties-of-silicon>, last accessed 2/25/2015
29. Ion, J.C.: *Laser Processing of Engineering Materials: Principles, Procedure and Industrial Application*. Elsevier, Butterworth-Heinemann (2005)
30. Chien, J., Pepiot, P., Khayms, V.: *Linear Algebra and Partial Differential Equations for Engineers. MATLAB Workbook*. Cornell University MATH2940 [http://www.learningace.com/doc/2716459/cfad8a2df94b9d7b954d3886ba22fd58/darve\\_cme104\\_matlab](http://www.learningace.com/doc/2716459/cfad8a2df94b9d7b954d3886ba22fd58/darve_cme104_matlab) last accessed 10/16/2015